Eidgenössische Technische Hochschule Zürich
Swiss Federal Institute of Technology Zurich

SED
Schweizerischer Erdbebendienst
Swiss Seismological Service

SED Extended Velocity Profiles at Rock Sites

Valerio Poggi, Jan Burjanek, Benjamin Edwards, Donat Fäh

Report SED/PRP/R/039/20130822

1 - Selection of the velocity profiles

Only rock sites from the stations of the Swiss seismic network have been selected that show no strong local resonances or strong polarization features of the wave-field (see chapter 5). Each raw velocity profile in the SED database ("MOD" folders) has been analyzed, and depths below the reliability limit have been manually removed from the models. Note that each site generally has a different maximum resolved depth, which depends on the employed investigation method (MASW, refraction seismics, ambient vibration array processing) and on the velocity structure of the site (which impacts the penetration depth of the wave-field during the investigation). The selection of the cutoff depth was quite conservative ("MOD_SEL" folders), to avoid issues when extending the velocity profile to large depths (see next section). See Table 1 for the list of cutoff depths for each site. Appendix 1 provides additional information such as kappa and the summary results from polarization analysis. Polarization analysis (Burjanek et al., 2013) and empirical amplification according to Edwards et al. (2013) are given in Appendix 2.

	Maximum depth	Resolved depth	Number of models
AIGLE	62 m	40 m	22
BALST	30 m	16 m	24
BNALP	34 m	20 m	20
BRANT	34 m	(no cut)	59
GIMEL	29 m	(no cut)	84
HASLI	35 m	(no cut)	41
LLS	18 m	12 m	30
PLONS	30 m	20 m	36
SIOV	40 m	40 m	50
SLUB	61 m	50 m	25
SULZ	26 m	15 m	46
SVIO	18 m	(no cut)	20
WIMIS	32 m	20 m	13

Table 1 - *Depths and number of models associated with each SED rock site.*

2 - Extending velocity profiles at the crustal reference

To refer the SED rock velocity profiles to a common crustal reference, each model has been extended to a depth of 4km ("MOD_EXT" folders) using a modification of the gradient rock reference model described in Poggi et al. (2011).

Practically, velocity at large depths has been extrapolated using the following functional form:

$$Vs(z) = (Vs_{max} - Vs_{min})\left[1 - b_1^{(-z/b_2)}\right] + Vs_{min}$$

where coefficients b_1, b_2 are curvature parameters and Vs_{min} and Vs_{max} are the velocity constraints of the lowermost reliable layer of the site and the average crustal velocity at the standard reference depth of 4000m respectively. The curvature coefficients and Vs_{max} correspond to those obtained in Poggi et al. (2011) (b_1 = 2.498, b_2 = 258.2223 and Vs_{max} = 3200m/s).

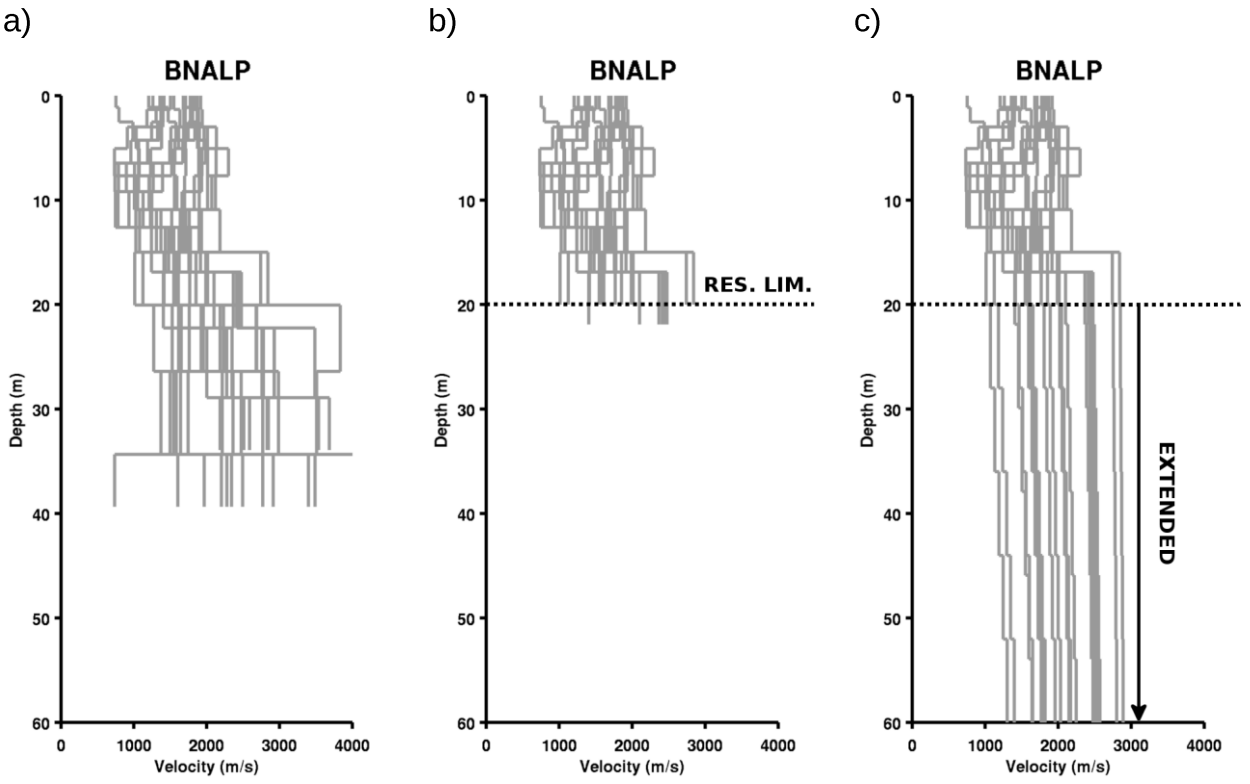

Figure 1 - *Example of the depth extension of a velocity model. a) Original raw model. b) Depth selection and cutoff. c) Extension to the reference depth of 4000m using a gradient model.*

3 - Average velocities

Average velocities over given depths are computed from the ensemble of all available models for each investigated sites ("LAB" folders). The calculation is done using the classic travel-time average approach (Vs-z) for the depths of 5, 10, 15, 20, 25, 30, 40, 50, 75 and 100m, and using the quarter-wavelength approach (Vs-qwl) over a frequency range of 0.25Hz to 50Hz.

For comparison, Vs-z values are also provided for the original raw models (PRP report TP2-TB-1019) and the selected profiles without extension (see folder common VSM and Table 2, Table 3, Table 4).

	Vs-5	Vs-10	Vs-15	Vs-20	Vs-25	Vs-30	Vs-40	Vs-50	Vs-75	Vs-100
AIGLE	1372	1347	1342	1318	1248	1228	1281	1404	1678	1846
BALST	1298	1287	1268	1265	1298	1348	1472	1561	1705	1792
BNALP	1574	1497	1465	1500	1580	1654	1778	1882	2062	2174
BRANT	901	825	867	947	1021	1079	1184	1260	1382	1453
GIMEL	1467	1392	1362	1399	1450	1496	1562	1606	1670	1704
HASLI	1535	1421	1400	1455	1534	1603	1722	1811	1949	2027
LLS	2920	2949	2911	2885	2958	3011	3081	3125	3187	3220
PLONS	1844	1770	1727	1742	1774	1810	1890	1943	2019	2060
SIOV	1036	1241	1406	1535	1506	1453	1524	1740	2215	2569
SLUB	701	709	845	952	1032	1094	1190	1305	1572	1752
SULZ	1162	1096	1065	1103	1144	1201	1285	1344	1435	1488
SVIO	1111	1111	1111	1111	1111	1111	1111	1111	1111	1111
WIMIS	1055	1119	1218	1311	1384	1443	1569	1664	1813	1900

Table 2 – *Travel-time average velocities versus depth from the raw velocity models of the SED sites (in gray the Vs-z which show some differences with the station monograph due to different profile selection procedures used for computing the average).*

	Vs-5	Vs-10	Vs-15	Vs-20	Vs-25	Vs-30	Vs-40	Vs-50	Vs-75	Vs-100
AIGLE	1372	1347	1342	1318	1248	1228	1281	1395	1585	1701
BALST	1298	1287	1268	1273	1290	1308	1338	1360	1397	1419
BNALP	1574	1497	1465	1500	1548	1589	1653	1700	1774	1817
BRANT	901	825	867	947	1021	1079	1184	1260	1382	1453
GIMEL	1467	1392	1362	1399	1450	1496	1562	1606	1670	1704
HASLI	1535	1421	1400	1455	1534	1603	1722	1811	1949	2027
LLS	2920	2949	2931	2924	2921	2919	2919	2918	2919	2919
PLONS	1844	1770	1727	1742	1766	1785	1812	1830	1858	1873
SIOV	1036	1241	1406	1535	1506	1453	1524	1704	2108	2416
SLUB	701	709	845	952	1032	1094	1190	1305	1571	1749
SULZ	1162	1096	1065	1097	1124	1146	1177	1198	1230	1247
SVIO	1111	1111	1111	1111	1111	1111	1111	1111	1111	1111
WIMIS	1055	1119	1218	1311	1384	1438	1516	1569	1649	1695

Table 3 - *Travel-time average velocities versus depth from selected/cutted velocity models of the SED sites.*

	Vs-5	Vs-10	Vs-15	Vs-20	Vs-25	Vs-30	Vs-40	Vs-50	Vs-75	Vs-100
AIGLE	1372	1347	1342	1318	1248	1228	1281	1397	1602	1740
BALST	1298	1287	1268	1277	1304	1332	1384	1429	1522	1598
BNALP	1574	1497	1465	1500	1554	1601	1679	1742	1857	1940
BRANT	901	825	867	947	1021	1079	1185	1268	1419	1527
GIMEL	1467	1392	1362	1399	1450	1496	1567	1621	1722	1799
HASLI	1535	1421	1400	1455	1534	1603	1722	1816	1972	2074
LLS	2920	2949	2931	2925	2924	2925	2929	2933	2944	2954
PLONS	1844	1770	1727	1742	1770	1794	1837	1872	1943	2002
SIOV	1036	1241	1406	1535	1506	1453	1524	1706	2110	2406
SLUB	701	709	845	952	1032	1094	1190	1305	1575	1761
SULZ	1162	1096	1065	1100	1136	1168	1222	1268	1361	1439
SVIO	1111	1111	1111	1111	1115	1124	1148	1175	1243	1309
WIMIS	1055	1119	1218	1311	1384	1440	1526	1592	1710	1797

Table 4 - *Travel-time average velocities versus depth from the extended velocity models of the SED sites.*

4 - Amplification functions

From the extended velocity profiles, amplification functions were derived using the elastic SH transfer function formalism and the quarter-wavelength approach (in “LAB” folders). Note that these amplification functions are all always with reference to the last layer of the models, which is 3200m/s at 4000m depth. The frequency range for the computation is 0.25Hz to 50Hz.

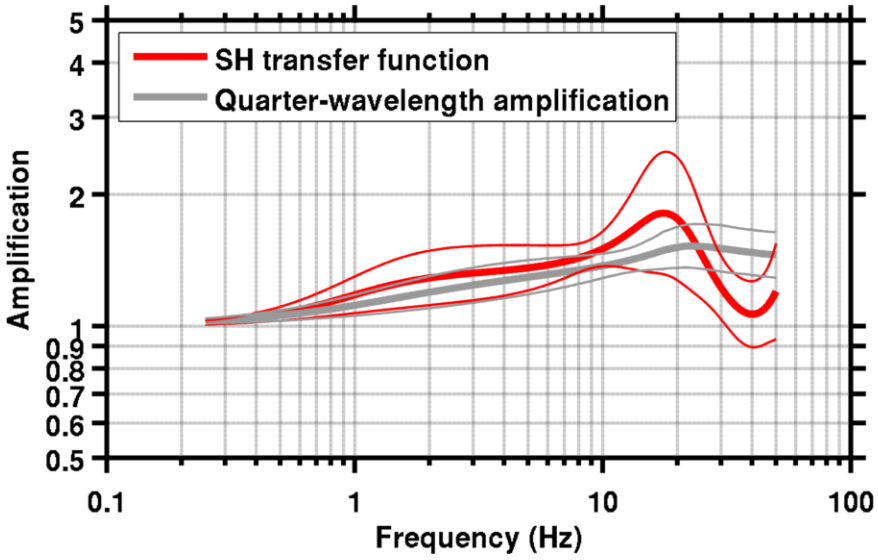

Figure 2 - *Example of extension of amplification function for the site BNALP.*

5 - Polarization analysis

Since a number of studies found directional site effects at rock sites (e.g., due to rock fracturing), we use the polarization analysis of particle motion as an additional element of ground motion characterization to select rock stations, as proposed in Burjanek et al. (2013). Results are given in Appendix 2 together with the empirical amplification according to Edwards et al. (2013). Time-frequency polarization analysis was performed on both earthquake and ambient vibration recordings. It is based on the combination of complex polarization analysis and the continuous wavelet transform. Three polarization parameters are retrieved: 1) azimuth of the major axis, or strike, measured in degrees from North; 2) tilt of the major axis, or dip, measured in degrees downward from the horizontal; and 3) ellipticity, defined as the ratio between the length of the semi-minor and semi-major axes. All three polarization parameters vary with both time and frequency. We analyze the relative occurrence of polarization parameters. In particular, histograms of polarization parameters are constructed over time for each frequency. Polar plots are then adopted for the presentation of final results, which illustrate combined angular and frequency dependence. The observed histograms of strike and dip can be fit for given frequency by the Wrapped Cauchy distribution which is characterized by its mean and concentration value. The frequency dependent level of directionality is then mapped to the frequency dependent concentration value ($\rho=0$ signifies no directionality, while $\rho\approx1$ means completely concentrated).

6 - References

Burjanek, J., Edwards, B., Fäh, D. 2013. Empirical evidence of topographic site effects: a systematic approach. Geophys. J. Int., submitted.

Edwards, B., C. Michel, V. Poggi and D. Fäh, 2013. Determination of Site Amplification from Regional Seismicity: Application to the Swiss National Seismic Networks. Seismological Research Letters Volume 84, Number 4, 611-621.

Poggi, V., B. Edwards and D. Fäh, 2011. Derivation of a Reference Shear-Wave Velocity Model from Empirical Site Amplification, Bull. seism. Soc. Am. 101, 258-274.

APPENDIX 1 – List of station parameters

Station (h=high, m=moderate, l=low)		V_S derived							Kappa		Polarization
Code	Quality	Vs 5	Vs 10	Vs 20	Vs 30	Vs 40	Vs 50	Vs 100	Kappa M2 Edwards	Kappa M1 Edwards	
AIGLE	l-m	1372	1347	1318	1228	1281	1397	1740	0.0142	0.0139	Moderate pol.4Hz (EW)
BALST	m	1298	1287	1277	1332	1384	1429	1598	0.0023	0.0028	flat
BNALP	m	1574	1497	1500	1601	1679	1742	1940	0.0142	0.015	flat
BRANT	m	901	825	947	1079	1185	1268	1527	0.0033	0.0041	Weak pol.25Hz (NS)
GIMEL	h	1467	1392	1399	1496	1567	1621	1799	0.0148	0.0144	flat
HASLI	m-h	1535	1421	1455	1603	1722	1816	2074	0.0077	0.0085	flat
LLS	l-m	2920	2949	2925	2925	2929	2933	2954	0.0025	0.0033	flat
PLONS	h	1844	1770	1742	1794	1837	1872	2002	0.0064	0.0069	flat
SIOV	l	1036	1241	1535	1453	1524	1706	2406	0.0162	0.0165	flat
SLUB	h	701	709	952	1094	1190	1305	1761	--	0.0257	flat
SULZ	h	1162	1096	1100	1168	1222	1268	1439	0.0136	0.0142	Weak pol.0.75Hz (NS)
SVIO	l	1111	1111	1111	1124	1148	1175	1309	--	0.0000	flat
WIMIS	l-m	1055	1119	1311	1440	1526	1592	1797	0.0102	0.0108	flat

NOTE: Cells in purple indicate the preferred kappa value (Station SLUB and SVIO do not include an M2 value due to a limitation in the algorithm implementation). Vs-Z values are from the extended profiles.

APPENDIX 2 – Polarization analysis of the SED sites

1st column: geometry of the terrain (based on ASTER GDEM) and location of the station (black cross). 2nd column: distribution of the strike angle. 3rd column: distribution of the ellipticity. 4th column: concentration vs. emprical amplification. Earthquake recordings are utilized for the polarization analysis, except stations SBUB and SLUB for which noise recordings of temporary stations were analyzed.

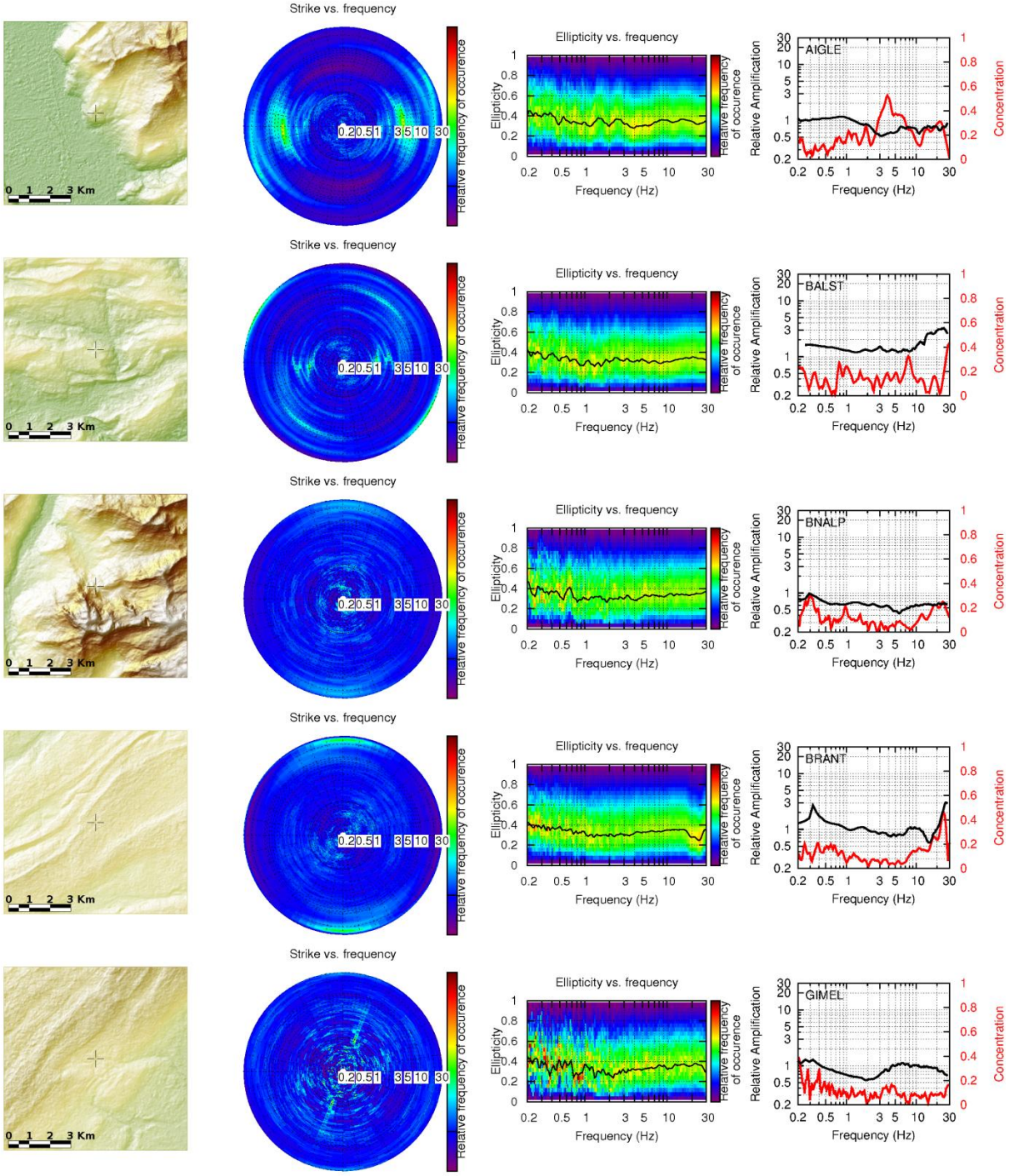

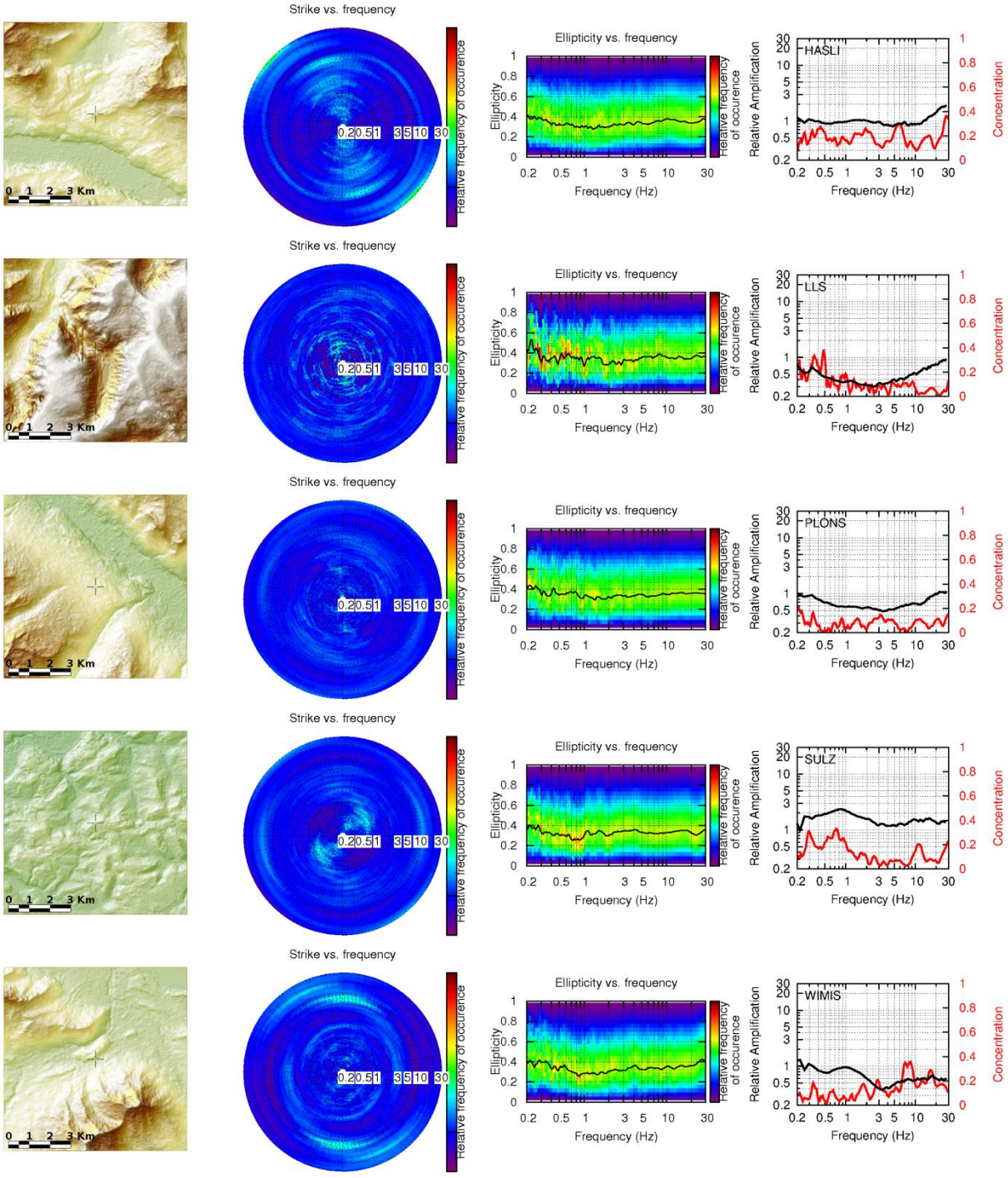
Strike vs. frequency
Relative frequency of occurence
0.2 0.5 1 3 5 10 30
0 1 2 3 Km
Ellipticity vs. frequency
Ellipticity
Frequency (Hz)
Relative Amplification
Concentration
HASLI
LLS
PLONS
SULZ
WIMIS

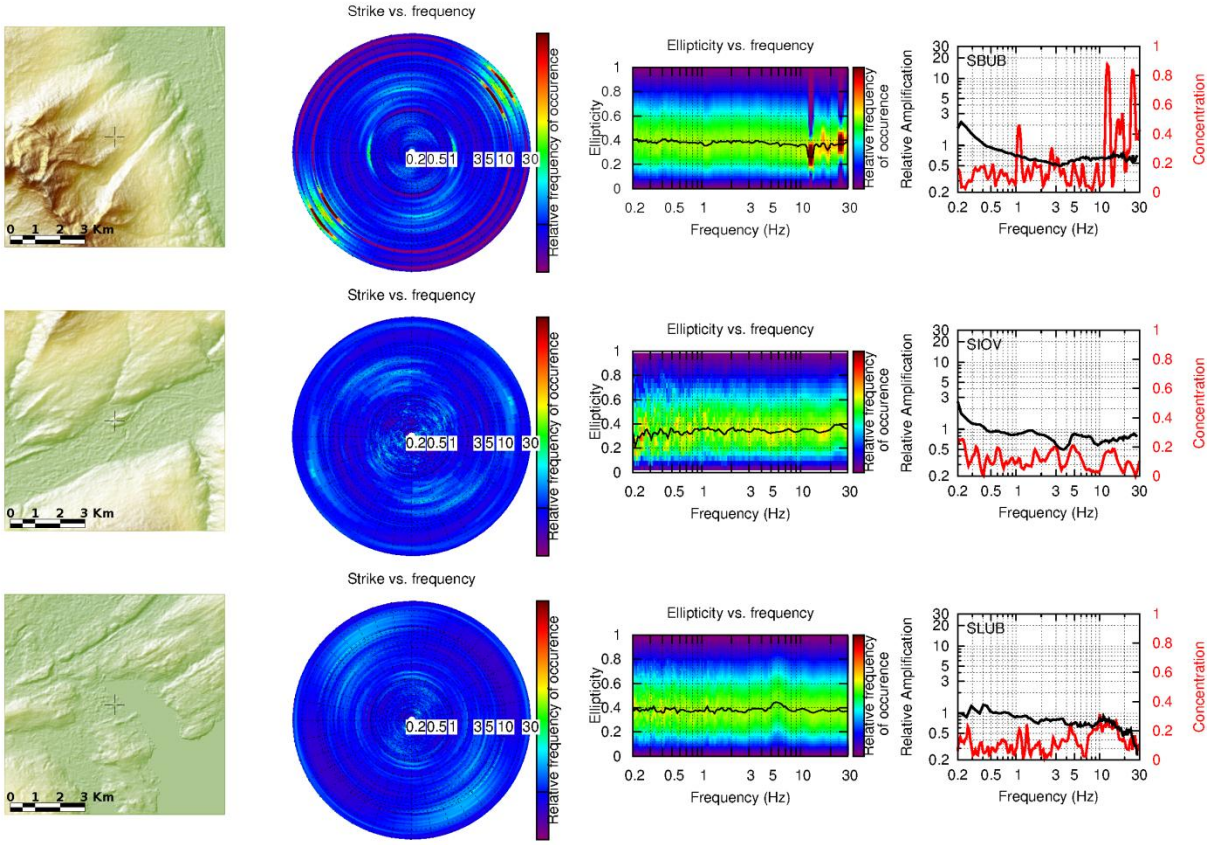
Strike vs. frequency
0 1 2 3 Km
0.2 0.5 1 3 5 10 30
Relative frequency of occurence
Ellipticity vs. frequency
Ellipticity
Relative frequency of occurence
Frequency (Hz)
Relative Amplification
SBUB
Concentration
Strike vs. frequency
0 1 2 3 Km
0.2 0.5 1 3 5 10 30
Relative frequency of occurence
Ellipticity vs. frequency
Ellipticity
Relative frequency of occurence
Frequency (Hz)
Relative Amplification
SIOV
Concentration
Strike vs. frequency
0 1 2 3 Km
0.2 0.5 1 3 5 10 30
Relative frequency of occurence
Ellipticity vs. frequency
Ellipticity
Relative frequency of occurence
Frequency (Hz)
Relative Amplification
SLUB
Concentration

APPENDIX 3 – QWL and SH amplification functions

1) AIGLE

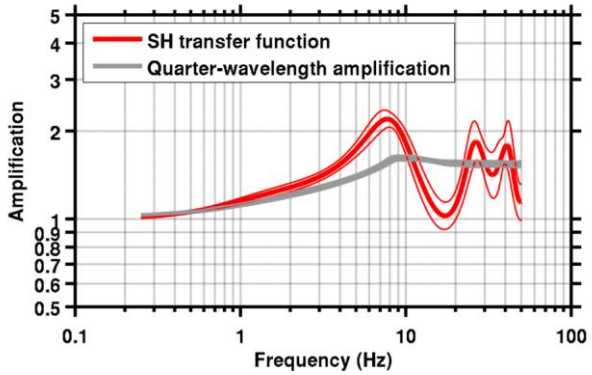

2) BALST

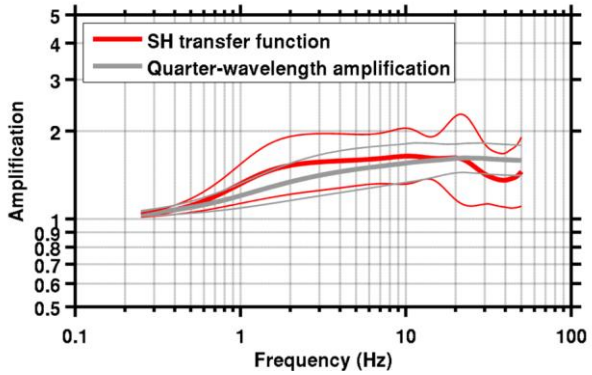

3) BNALP

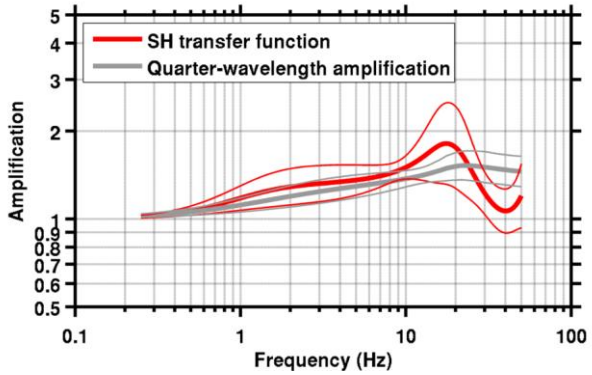

4) BRANT

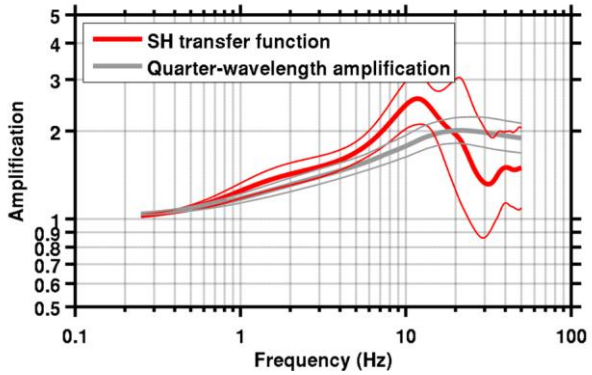

5) GIMEL

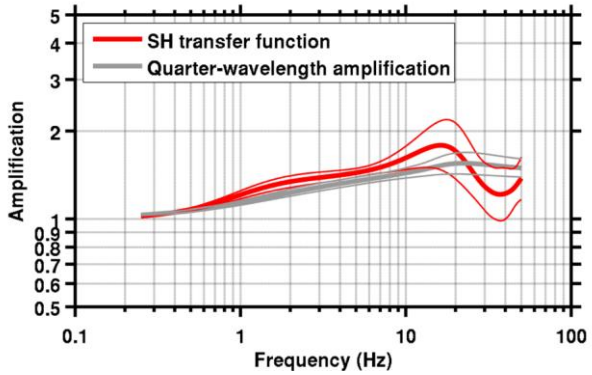

6) HASLI

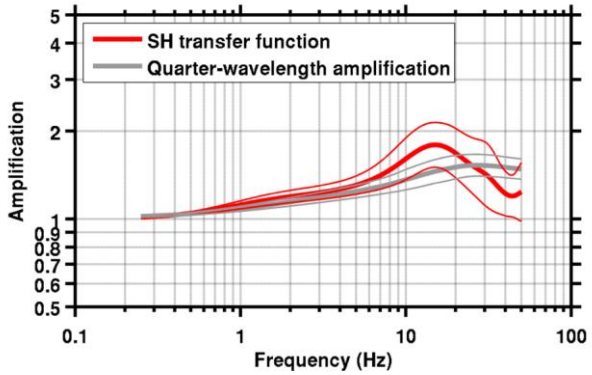

7) LLS

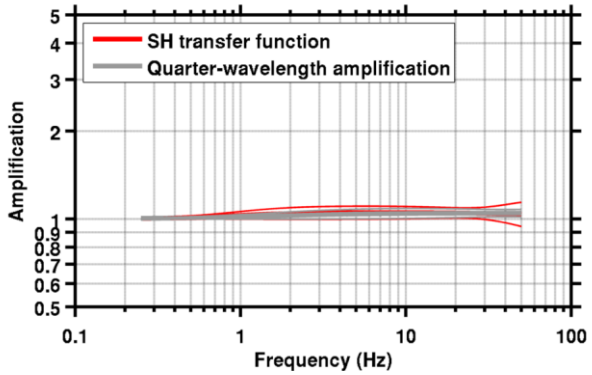

8) PLONS

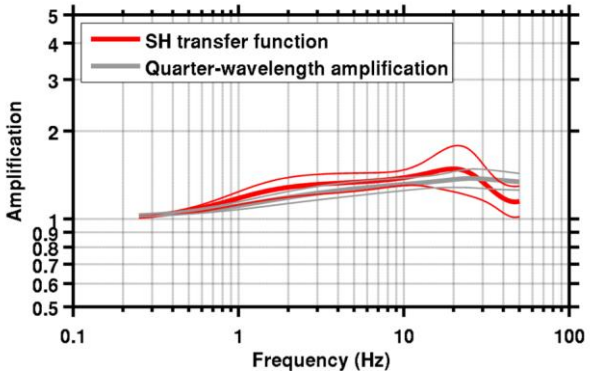

9) SIOV

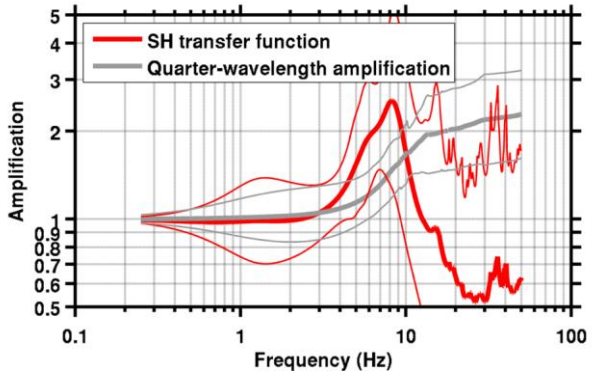

10) SLUB

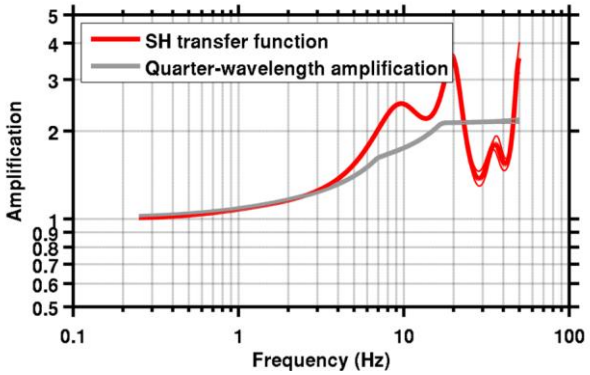

11) SULZ

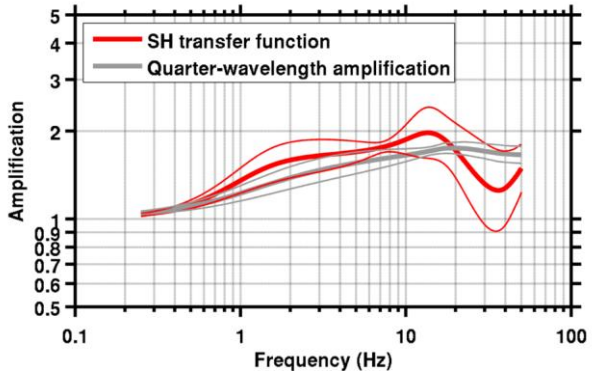

12) SVIO

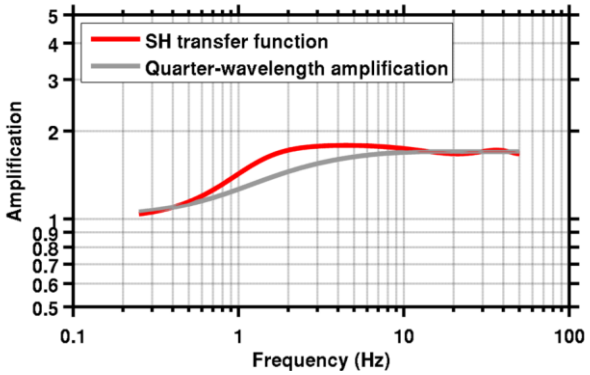

13) WIMIS

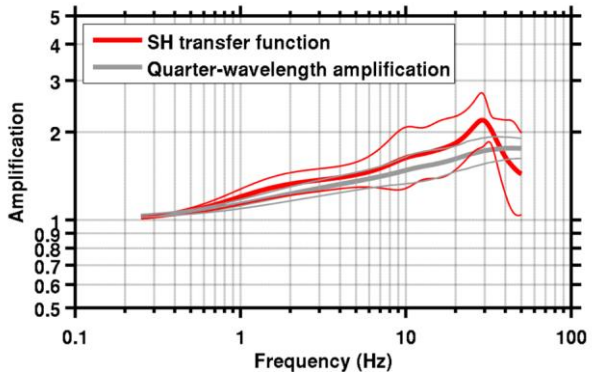
SH transfer function
Quarter-wavelength amplification
Amplification
Frequency (Hz)
5
4
3
2
1
0.9
0.8
0.7
0.6
0.5
0.1
1
10
100